Ion Pairs of Weakly Coordinating Cations and Anions: Synthesis and Application for Sulfide to Sulfoxide Oxidations

Bo Zhang[a], Su Li[a], Mirza Cokoja[a], Eberhardt Herdtweck[a], János Mink[b], Shu-Liang Zang[c], Wolfgang A. Herrmann[a], and Fritz E. Kühn[a]

[a] Chair of Inorganic Chemistry/Molecular Catalysis, Catalysis Research Center, Technische Universität München, Ernst-Otto-Fischer-Straße 1, D-85747 Garching bei München, Germany

[b] Institute of Molecular Pharmacology, Research Centre for Natural Sciences, Hungarian Academy of Sciences, Budapest, H-1525 Hungary; Faculty of Information Technology, University of Pannonia, Research Institute of Chemical and Process Engineering, Veszprém, H-8201, Hungary

[c] Department of Petroleum and Chemical Technology, Liaoning University of Petroleum and Chemical Technology, Dandong Road, No. 1, 113001 Fushun, P. R. China; Institute of Rare and Scattered Elements Chemistry, Liaoning University, Chongshan Middle Road No. 66, 110036 Shenyang, P. R. China

Reprint requests to Prof. Dr. F. E. Kühn. Tel: +49 89 289 13096. Fax: +49 89 289 13473.
E-mail: fritz.kuehn@ch.tum.de

Z. Naturforsch. **2014**, *69b*, 1149 – 1163 / DOI: 10.5560/ZNB.2014-4165
Received July 31, 2014

Dedicated to Professor Hubert Schmidbaur on the occasion of his 80th birthday

A series of salts containing the weakly coordinating cations (WCC) 1-butyl-3-methylimidazolium ($[Bmim]^+$), 1-butyl-2,3-dimethylimidazolium ($[Bdmim]^+$), 1-dodecyl-3-methylimidazolium ($[C_{12}mim]^+$), tetrabutylphosphonium ($[PBu_4]^+$), tributyltetradecylphosphonium ($[P_{4,4,4,14}]^+$), tetrabutylammonium ($[NBu_4]^+$), and 1,1,3,3-tetramethylguanidium ($[TMG]^+$) and fluorinated tetraarylborate anions of the type $[B(Ar^F)_4]$ ($Ar^F = C_6F_5$, C_6H_3-3,5-$(CF_3)_2$) were synthesized and characterized. The influence of cations and anions on the physical properties of the obtained compounds was examined. In case of the compound $[TMG][B(C_6F_5)_4]$ hydrogen-fluorine contacts between cation and anion are present in the solid state. Owing to H···F contacts between hydrogen peroxide and the fluorine substituents of the anion and the resulting activation of H_2O_2 in solution, the compound $[P_{4,4,4,14}][B(C_6H_3\text{-}3,5\text{-}(CF_3)_2)_4]$ is applicable as an efficient mediator for the oxidation of sulfides to sulfoxides.

Key words: Weakly Coordinating Anion, Hydrogen Peroxide, Oxidation, Sulfide, Sulfoxide

Introduction

The growing importance of environmental issues for society and industry during the past few decades has led to increasing attention to the need for more environmentally friendly and more sustainable technologies in chemical industry [1 – 8]. Minding this background, ionic liquids (IL) have been regarded as promising reaction media, as they are often non-toxic and not volatile. Yet, most importantly, they can be tailor-made to achieve desired properties, *e. g.* high hydrophobicity and concomitant high polarity, thus offering a large variety of compounds with different cations and anions [9 – 17]. It is therefore not surprising that ILs play an important role in recent examinations aiming at "green" chemistry and applications in catalysis [3, 4, 7, 9, 18 – 23] The degree of ion pairing interactions and the size and charge distribution of the ions influence the melting point, viscosity and conductivity [20, 24, 25]. The ion pairing interactions can be ascribed to the strength of different bonding types between the ions, mainly Coulomb forces and hydrogen contacts, which depend on the Lewis basicity of the anions [26 – 34]. For this reason, ion pairs containing weakly coordinating cations (WCC; *e. g.* ammonium, phosphonium, pyri-

© 2014 Verlag der Zeitschrift für Naturforschung, Tübingen · http://znaturforsch.com

dinium, imidazolium) and weakly coordinating anions (WCA; *e. g.* $[BF_4]^-$, $[PF_6]^-$, $[AlCl_4]^-$, $[CF_3SO_3]^-$, $[N\{SO_2(CF_3)\}_2]^-$) are among the best studied IL systems [35, 36], as they exhibit weak Coulomb (owing to charge delocalization) and weak hydrogen bonding interactions [1 – 3]. For example, ILs consisting of $[Al(OR^F)_4]^-$ ($R^F = C(CF_3)_3$, $C(H)(CF_3)_2$, $C(CH_3)(CF_3)_2$, $C(Ph)(CF_3)_2$) anions associated with imidazolium cations have been described and applied as solvents for electrochemical and catalytic applications [37 – 40]. Matsumoto *et al.* prepared and characterized low-melting and low-viscous ILs with perfluoroalkyltrifluoroborates [41 – 44]. A comprehensive examination of ionic compounds based on carborane [45 – 47] or azolate [48, 49] anions was also performed. However, in terms of anion stability, it has been shown that weakly coordinating fluorinated tetraarylborate $[B(Ar^F)_4]^-$ anions ($Ar^F = C_6F_5$, $-C_6H_3$-3,5-$(CF_3)_2$) are much more stable than the above mentioned anions [50 – 54]. Therefore, $[B(Ar^F)_4]^-$ anions are widely used as counterions for a plethora of cationic catalysts, *e. g.* for the polymerization of olefins [55 – 58].

Recently it has been demonstrated that a reduced ion pairing interaction leads to an increased nucleophilicity of perrhenate [59, 60] and polyoxomolybdate [61, 62] anions, rendering anion-based activation of H_2O_2 and oxidation of olefins and sulfides possible. Additionally, the synthesis of imidazolium salts containing the $[B(C_6F_5)_4]^-$ anion showing a weak cation-anion interaction was reported [63]. The tetrafluoroborate anion is also capable of activating hydrogen peroxide by forming hydrogen bonds, which leads to the oxidation of sulfides [65]. These findings led to the idea of synthesizing several different ionic compounds with weakly coordinating cations and fluoride-containing weakly coordinating anions (WCCWCA), and investigating the relationship between the structure and the resulting physical properties. In this work a series of WCCWCAs, prepared by combining the organic cations (1-butyl-3-methylimidazolium ($[Bmim]^+$), 1-butyl-2,3-dimethylimidazolium ($[Bdmim]^+$), 1-dodecyl-3-methylimidazolium ($[C_{12}mim]^+$), tetrabutylphosphonium ($[PBu_4]^+$), tributyltetradecylphosphonium ($[P_{4,4,4,14}]^+$), tetrabutylammonium ($[NBu_4]^+$), and 1,1,3,3-tetramethylguanidium ($[TMG]^+$)) with two different $[B(Ar^F)_4]^-$ anions ($Ar^F = C_6F_5$, $-C_6H_3$-3,5-$(CF_3)_2$) is described. In analogy to our previous studies [62, 64], some of the new WCCWCAs were applied as mediators for the oxidation of sulfides to sulfoxides. Oxidation of sulfur-containing compounds is of considerable current interest for industrial chemistry and petrochemistry [65 – 69].

Results and Discussion

Synthesis and characterization

The WCCWCAs were synthesized according to modified literature procedures [64]. They can be accessed *via* salt metathesis from WCC-halide salts and either lithium- or silver-WCAs, as shown in Scheme 1. $Li[B(C_6F_5)_4]$ and $Li[B\{C_6H_3$-3,5-$(CF_3)_2\}_4]$ were synthesized according to literature procedures [64, 70]. WCCWCAs **1a**–**7a** and **1b**–**7b** are obtained by the reaction of $Li[B(C_6F_5)_4]$ or $Li[B\{C_6H_3$-3,5-$(CF_3)_2\}_4]$ with WCC halides in dry CH_2Cl_2 under argon atmosphere with a reaction time of 2 h at room temperature. After precipitation of the by-product and filtration of the product-containing supernatant, the solvent is removed under vacuum. The remaining product is washed with dry pentane, and dried under high vacuum for one day. The yields of the purified products are 55 – 62 %. In order to increase the yield and reduce the reaction time, $Ag[B(C_6F_5)_4]$ and $Ag[B\{C_6H_3$-3,5-$(CF_3)_2\}_4]$ have been selected as precursors for the synthesis of the WCCWCAs. $Ag[B(C_6F_5)_4]$ and $Ag[B\{C_6H_3$-3,5-$(CF_3)_2\}_4]$ were prepared according to literature procedures [71]

The reaction is carried out under exclusion of light at room temperature in dry CH_2Cl_2. The reaction mixture is stirred for 10 min, while the by-product precipitates. After filtration, the solvent is removed under high vacuum to obtain the raw product. This raw product is then washed with dry pentane and dried under vacuum for one day. Typical yields of the pure products are 85 – 95 %. Hence, the best results are usually obtained with silver salts rather than lithium salts in dry dichloromethane. All prepared WCCWCAs are stable to air and moisture. All synthesized compounds are solid at room temperature, with the exception of **6a**, which is a pale-yellow liquid with a melting point of –39°C (see Table 1). All salts display high solubility in water and polar organic solvents such as CH_2Cl_2, CH_3CN and alcohols, but low solubility in *n*-hexane.

The WCCWCAs **1a**–**7a** and **1b**–**7b** have been characterized by FT-IR, NMR spectroscopy and elemental analysis (see the Experimental Section). Melting

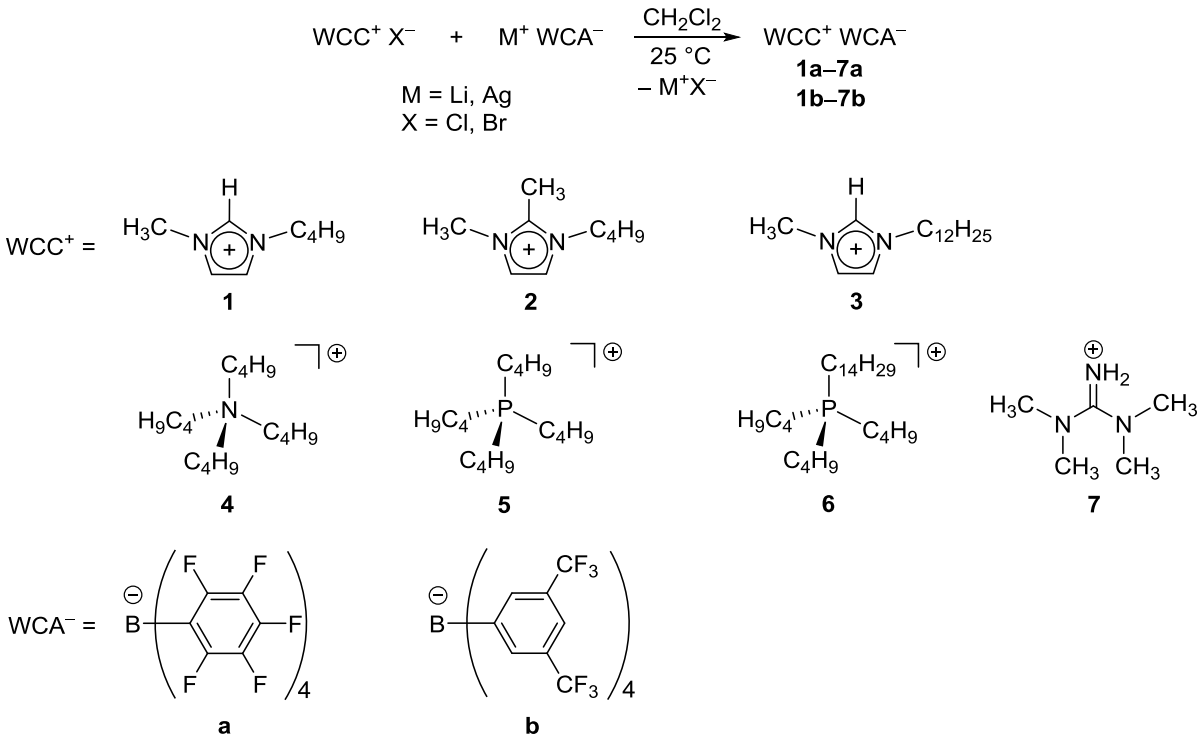

Scheme 1. Synthesis of WCCWCA compounds **1a**–**7a** and **1b**–**7b**.

points (T_m) were determined by differential scanning calorimetry (DSC). The results are summarized in Table 1. Note that the melting points of WCCWCAs with the $[B\{C_6H_3\text{-}3,5\text{-}(CF_3)_2\}_4]$ anion (**1b**–**7b**) are significantly lower than those with the $[B(C_6F_5)_4]^-$ anion (**1a**–**7a**), indicating that the size of the anion affects the ion pairing and hence the long-range order [72]. The nature of the cation, however, also influences the melting point, as shown with the $[P_{4,4,4,14}]^+$ cation, which is giving rise to the long tetradecyl chain and hence, the lowest melting points in the series of the synthesized WCCWCAs, being –39°C for **6a** and 49°C for **6b**. In contrast, WCCWCAs with cations of high T_d symmetry (**4** and **5**) lead to higher melting points. It is reported that symmetry breaking in cations leads to lower melting points of ionic liquids [73]. Similarly, the melting points of **2a** and **2b** decrease with increasing length of the alkyl chain from butyl to dodecyl due to increasing cation size and decreasing cation symmetry. Generally, WCCWCAs with cations exhibiting acidic protons (imidazolium, guanidinium) have higher melting points than those with ammonium and phosphonium cations, owing to hydrogen bonding between cation and anion, which is known to have an influence on the melting point (see also the crystal structures below) [24 – 26, 74 – 76].

The thermal stability of compounds **1a**–**7a** and **1b**–**7b** was determined by thermogravimetric analyses (TGA), with isocratic heating at 10°C min^{-1} under an

Table 1. Decomposition temperatures T_d and melting points T_m of the synthesized WCCWCAs.

Entry	Compound	T_d (°C)	T_m (°C)
1	$[Bmim][B(C_6F_5)_4]$ (**1a**)	245	145
2	$[Bdmim][B(C_6F_5)_4]$ (**2a**)	270	151
3	$[C_{12}mim][B(C_6F_5)_4]$ (**3a**)	287	120
4	$[NBu_4][B(C_6F_5)_4]$ (**4a**)	220	159
5	$[PBu_4][B(C_6F_5)_4]$ (**5a**)	330	114
6	$[P_{4,4,4,14}][B(C_6F_5)_4]$ (**6a**)	337	–39[a]
7	$[TMG][B(C_6F_5)_4]$ (**7a**)	255	152
8	$[Bmim][B\{C_6H_3\text{-}3,5\text{-}(CF_3)_2\}_4]$ (**1b**)	260	106
9	$[Bdmim][B\{C_6H_3\text{-}3,5\text{-}(CF_3)_2\}_4]$ (**2b**)	255	91
10	$[C_{12}mim][B\{C_6H_3\text{-}3,5\text{-}(CF_3)_2\}_4]$ (**3b**)	284	73
11	$[NBu_4][B\{C_6H_3\text{-}3,5\text{-}(CF_3)_2\}_4]$ (**4b**)	238	92
12	$[PBu_4][B\{C_6H_3\text{-}3,5\text{-}(CF_3)_2\}_4]$ (**5b**)	300	121
13	$[P_{4,4,4,14}][B\{C_6H_3\text{-}3,5\text{-}(CF_3)_2\}_4]$ (**6b**)	318	49
14	$[TMG][B\{C_6H_3\text{-}3,5\text{-}(CF_3)_2\}_4]$ (**7b**)	250	156

[a] Glass transition temperature.

inert argon atmosphere. All WCCWCAs are thermally stable beyond 240°C (Table 1). The decomposition points also appear to mainly depend on the structure of the anion. With longer alkyl substituents at the cation, the decomposition temperature increases. Phosphonium WCCWCAs show higher thermal stability than the corresponding imidazolium salts. Previous reports have shown that salt compounds containing WCAs **a** and **b** and cationic transition metal complexes usually decompose below 200°C [77 – 79], indicating that the WCCWCAs display increased thermal stability.

Crystal structure analysis

Single crystals of **2b**, **5a**, **6b**, and **7a** were obtained by slow diffusion of *n*-hexane into a dichloromethane solution of the compounds at –10°C. The diffraction measurements were carried out at low temperatures (between 100 and 200 K) in order to minimize rotation of the CF_3 groups and ensure the accuracy of the evaluation of intermolecular interactions involving F and H atoms.

Compound **2b** crystallizes in the monoclinic space group $P2_1/c$ with $Z = 4$ (Fig. 1). Noteworthy, there are no significant cation-anion contacts, which is giving rise to the substitution of a hydrogen atom at the C2 ring position by a methyl group (*c.f.* [Bmim][$B(C_6F_5)_4$] (**1a**) [64]. This is in good agreement to previous observations that hydrogen bonds become less pronounced when the H atoms on the imidazolium ring are replaced by alkyl groups [28].

Compound **5a** crystallizes in the orthorhombic space group $Pca2_1$ with two molecules per unit cell. The asymmetric unit consists of two $[PBu_4]^+$ ions and two $[B(C_6F_5)_4]^-$ ions (Fig. 2). Expectedly, the B–C bond lengths (1.656(2) – 1.664(2) Å) are in a similar range as the B–C bond lengths (1.657(4) – 1.681(4) Å) of the similar structure $[NBu_4][B(C_6F_5)_4]$ described

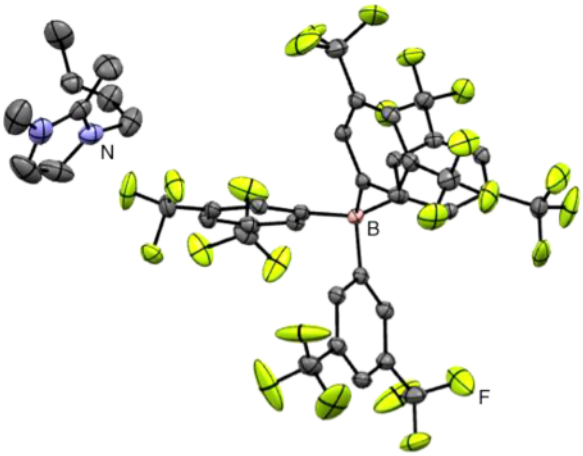

Fig. 1. (color online). ORTEP view of the solid-state structure of compound **2b**. Displacement ellipsoids are drawn at the 50 % probability level. Hydrogen atoms are omitted for clarity. Atom colors: carbon: grey, nitrogen: blue, boron: pink, fluorine: green.

by M. Bolte *et al.* [80]. The bond lengths and angles are listed in Table 2. H···F contacts between the *ortho*-fluorine atoms and the γ- and δ-carbon atoms of the butyl substituents are visible.

Compound **6b** crystallizes in the triclinic space group $P\bar{1}$ with $Z = 2$. The structure is shown in Fig. 3, and the crystallographic data are summarized in the Experimental Section. Interestingly, in comparison to compound **5a**, there are significantly less H···F contacts in compound **6b**, which is most presumably a consequence of the steric repulsion of the tetradecyl group and the different basicities of fluorine atoms in CF_3 and C_6F_5 groups. The bond angle $(C–B–C)_{min}$ (107.5(1)°) is larger than that of other compounds containing the $[B(C_6F_5)_4]^-$ anion, probably due to the steric hindrance of the longer carbon chain of the cation.

Table 2. Comparison of selected bond lengths (Å) and angles (deg).

Entry	Compound	Bond lengths (B–C) (min–max) (Å)	Bond angles (C–B–C) (min–max) (deg)
1	[Bmim][$B(C_6F_5)_4$] (**1a**)	1.652(2) – 1.655(2) [64]	101.3(1) – 114.6(1) [64]
2	[Bdmim][$B(C_6F_5)_4$] (**2a**)	1.653(3) – 1.659(3) [64]	101.2 (1) – 114.2(2) [64]
3	[NBu_4][$B(C_6F_5)_4$] (**4a**)	1.657(4) – 1.681(14) [81]	100.5(2) – 115.5(2) [81]
4	[$PBu_{,4}$][$B(C_6F_5)_4$] (**5a**)	1.656(2) – 1.664(2)	101.4(1) – 115.6(1)
5	[TMG][$B(C_6F_5)_4$] (**7a**)	1.39(2) – 1.661(2)	102.3(1) – 113.3(1)
6	[Dbmim][$B\{C_6H_3$-3,5-$(CF_3)_2\}_4$] (**2b**)	1.635(2) – 1.640(2)	101.9(2) – 122.7(1)
7	[$P_{4,4,4,14}$][$B\{C_6H_3$-3,5-$(CF_3)_2\}_4$] (**6b**)	1.649(2) – 1.65(2)	107.5(1) – 111.1(1)

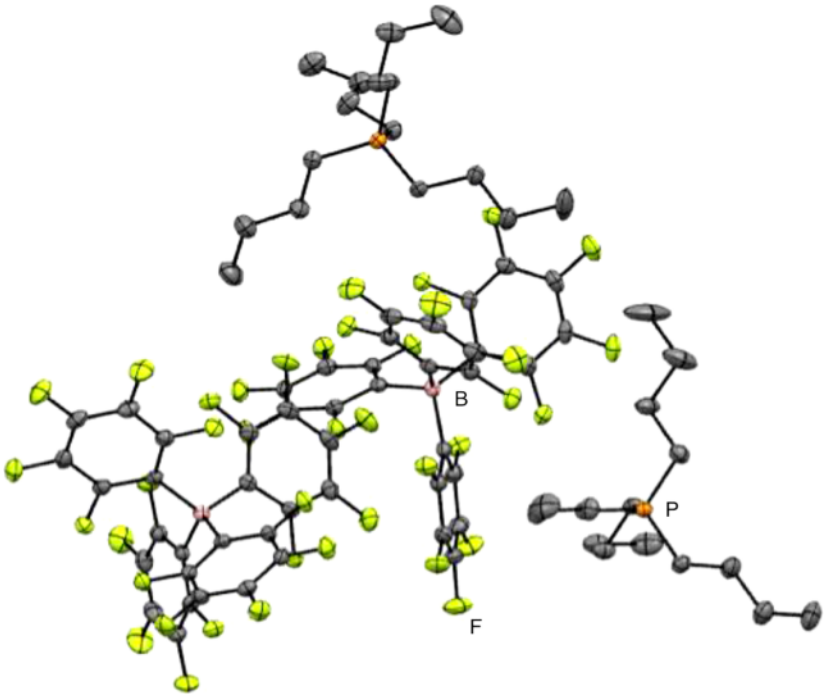

Fig. 2. (color online). ORTEP view of the solid-state structure of compound **5a**. Displacement ellipsoids are drawn at the 50 % probability level. Hydrogen atoms are omitted for clarity. Atom colors: carbon: grey, phosphorus: orange, boron: pink, fluorine: green.

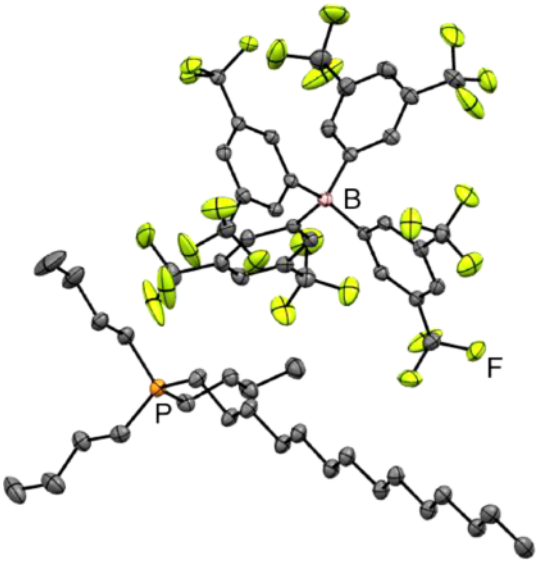

Fig. 3. (color online). ORTEP view of the solid-state structure of compound **6b**. Displacement ellipsoids are drawn at a 50 % probability level. Hydrogen atoms are omitted for clarity. Atom colors: carbon: grey, phosphorus: orange, boron: pink, fluorine: green.

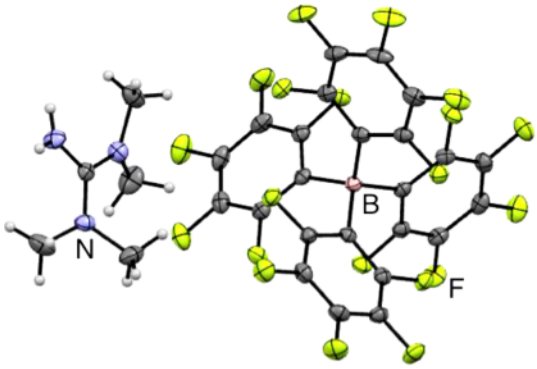

Fig. 4. (color online). ORTEP view of the solid-state structure of compound **7a**. Displacement ellipsoids are drawn at a 50 % probability level. Atom colors: carbon: grey, nitrogen: blue, boron: pink, fluorine: green.

Compound **7a** crystallizes in the triclinic space group $P\bar{1}$ with $Z = 2$ (Fig. 4). It is noteworthy that hydrogen atoms could be located in the difference Fourier maps and are allowed to refine freely. In the solid state, compound **7a** exhibits a plethora of

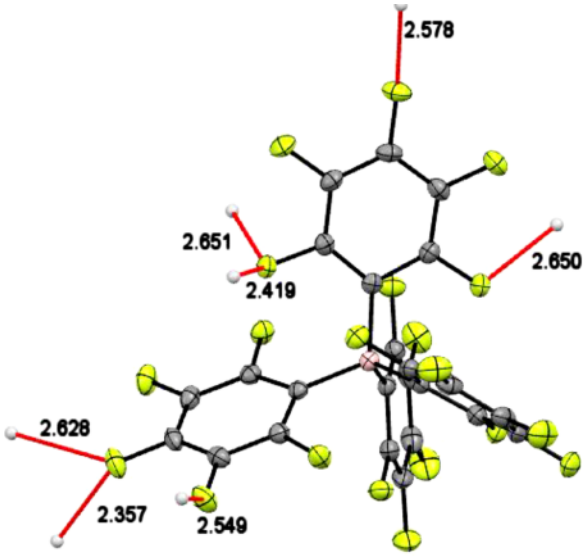

Fig. 5. (color online). Illustration of hydrogen contacts (in red color) of the fluoride groups of the $[B(C_6F_5)_4]^-$ anion in **7a**.

hydrogen-bonding interactions between the F atoms of $[B(C_6F_5)_4]^-$ and the hydrogen atoms of the 1,1,3,3-tetramethylguanidinium (TMG) cation (Fig. 5). The length of the hydrogen bonds is in the range of 2.357 to 2.650 Å, respectively, which is in the range of typical H···F contacts [81 – 85]. The pronounced interactions between cation and anion *via* hydrogen bonds may be attributed to the relative acidity of the protons of the TMG cation.

Oxidation of sulfides to sulfoxides mediated by WCCWCAs

In analogy to the oxidation of sulfides to sulfoxides mediated by imidazolium tetrafluoroborates, the oxidation of sulfides to sulfoxides was carried out using compounds **6a** and **6b** as reaction media, since they exhibit the lowest melting points in the series of all synthesized WCCWCAs. Oxidation of thioanisole with aqueous H_2O_2 as the oxidant was found to be strongly solvent dependent (details concerning the reaction details are given in the Experimental Section). When using **6a** as solvent, the sulfoxide yield is only 18 % within 4 h with a selectivity of 90 %. In an analogous experiment using **6b** nearly quantitative conversion and selectivity were obtained after the same reaction time (see Fig. 6). Therefore, for subsequent oxidation experiments, **6b** was chosen as the medium for the oxidation of sulfides to sulfoxides with H_2O_2 at room temperature (Scheme 2). A blank experiment without oxidant was also investigated. No considerable oxidation was observed within 24 h, indicating that the oxygen source for the synthesis of sulfoxide is not air. Maximum yield is achieved after 4 h reaction time, while the selectivity remains unchanged during the whole reaction time.

To generalize the developed methodology, the oxidation of various sulfides with different substituents was examined. The results are shown in Table 3. All sulfides are effectively oxidized to the corresponding sulfoxides in good to excellent yields using 35 % aqueous hydrogen peroxide at room temperature. Interestingly, dialkyl sulfides (entries 2, 3) are more active, affording very high sulfoxide yields (within 3 h). Diaryl sulfides (entries 1, 3 – 7) are less efficiently oxidized, probably due to steric hindrance. The electronic nature of the substituents has less influence on the yield and selectivity of the sulfoxide products (entries 4 – 7) in the oxidation of various phenyl-substituted sulfides to the corresponding sulfoxides. It is important to note that another useful feature of the presented protocol

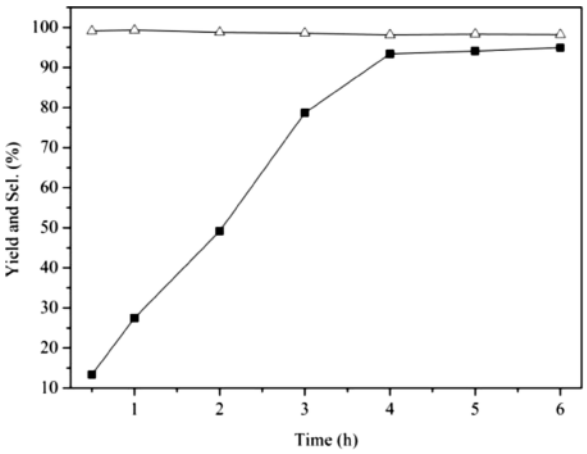

Fig. 6. Time-dependent yield (■) and selectivity (△) of methyl phenyl sulfoxide.

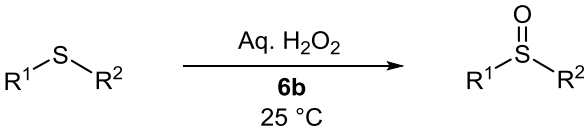

Scheme 2. Oxidation of sulfides to sulfoxides mediated by WCCWCA **6b**.

Table 3. Oxidation of sulfides to sulfoxides with aqueous H_2O_2 mediated by WCCWCA **6b**[a].

Entry	R^1	R^2	Time (h)	Yield[b] (%)	Selectivity[c] (%)
1	Ph	Me	4	93	97
2	Me	Me	3	94	98
3	*n*-Butyl	*n*-Butyl	4	91	97
4	Ph	Ethyl	5	84	96
5	Ph	$CH(CH_3)_2$	5	80	97
6	Ph	$CH_2CH{=}CH_2$	6	82	96
7	Ph	CH_2CH_2OH	5	86	97

[a] Reaction conditions: 0.5 mL **6b**, 2 mmol substrate, 5 mmol H_2O_2 (30 %) at 25 °C; [b] isolated yield after column chromatography; [c] determined by GC-MS or ^{1}H NMR spectroscopy of the crude reaction mixture.

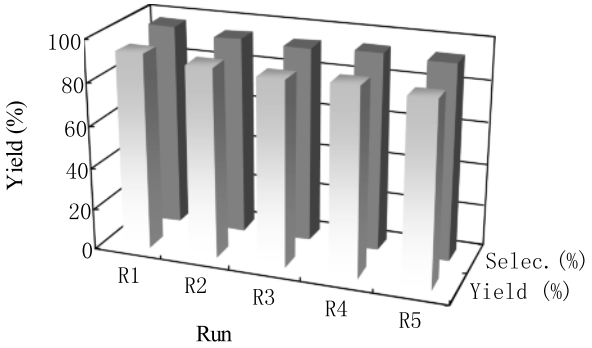

Fig. 7. Oxidation of thioanisole with H_2O_2 in **6b** at 25 °C after five reaction cycles.

is that neither epoxidation of the double bond of allyl phenyl sulfide (entry 6) nor oxidation of the hydroxy group (entry 7) is observed.

The advantage of this oxidation system is the recycling of the WCCWCA. After reaction completion, the product is extracted with *n*-hexane-diethyl ether, and subsequently, **6b** is extracted with CH_2Cl_2. The obtained liquid is dried over anhydrous $MgSO_4$ and then dried under high vacuum. Five recycling tests were carried out. The results are summarized in Fig. 7. No significant loss of yield and selectivity was observed after five runs of thioanisol oxidation. This system provides an advantage with respect to recycling and stability when compared to the other systems, which use organic solvents as media for the oxidation of sulfides [86 – 88].

Regarding the mechanism of this reaction, the interaction between the anion of **6b**, H_2O_2 and H_2O appears to be crucial. It is known that organic sulfides are oxidized by hydrogen peroxide in a heterolytic process involving nucleophilic attack of the sulfur on the oxygen atom [89]. This also explains why dialkyl sulfides are more easily oxidized than diaryl sulfides. The efficiency of the described oxidizing system can be explained by a specific feature of **6b**, which not only acts as solvent but also can be regarded as a promoter of the organic reaction [65]. Because of the electron-withdrawing character of the CF_3 group, a hydrogen bond between the fluoride substituents of the $[B\{C_6H_3\text{-}3,5\text{-}(CF_3)_2\}_4]^-$ anion in **6b** and H_2O_2 or H_2O is formed and prevents any further oxidation to sulfone [90]. Furthermore, the $[B\{C_6H_3\text{-}3,5\text{-}(CF_3)_2\}_4]^-$ anion is more stable under oxidative conditions than ionic liquids containing $[BF_4]^-$ or $[PF_6]^-$ anions, which are sensitive to hydrolysis and release of hydrofluoric acid [91 – 95].

IR spectroscopy

In order to further study the interactions between the WCCWCA **6b** and H_2O/H_2O_2 IR and NMR spectroscopy experiments were carried out. For an understanding of the hydrogen bonding to fluoride, D_2O was applied in the IR measurements. Figs. 8 and 9 show the IR spectra of the C–F stretching region of **6b** in D_2O and H_2O_2. The CF_3 stretching modes are very prominent in the infrared spectra. The local C_{3v} symmetry should produce only two bands; a higher asymmetric (ν_a) and lower symmetric (ν_s) stretching vibration. Instead, three pronounced bands at 1355, 1275 and 1119 cm^{-1} are observed. The first two bands can be interpreted as individual localized CF stretching vibrations, showing different CF bond lengths. The broad band near 1119 cm^{-1} appears to be a symmetric stretching mode of different, overlapping CF bands ($\nu > \nu' > \nu$). This explanation is in agreement with literature data on previously described organic CF_3 derivatives [96 – 104]. While ν and ν' are not shifted, new bands are formed in the region of the CF_3 symmetric stretching mode (Fig. 8). The second derivatives of the original spectra are shown in Fig. 9. When adding D_2O or H_2O_2 to **6b**, two new bands at 1115 and 1124 cm^{-1} or 1114 and 1123 cm^{-1} are formed, respectively. Furthermore, the development of a shoulder near 1085 cm^{-1} can be seen in Fig. 8, spectra 2a and 3a. In Fig. 9, the band at 1085 cm^{-1} in 2b and 3b is getting stronger compared to the pure ionic liquid. These changes can be ascribed to a further distortion of the CF_3 local symmetry from C_{3v} to C_1 leading to

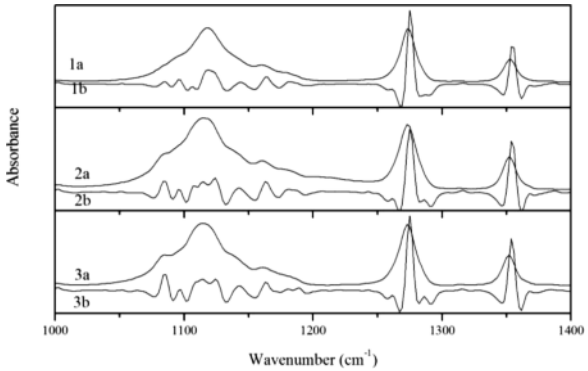

Fig. 8. C–F stretching region of neat **6b** (1a,1b), a mixture of **6b** and D_2O (2a, 2b) and a mixture of **6b** and H_2O_2 (3a, 3b).

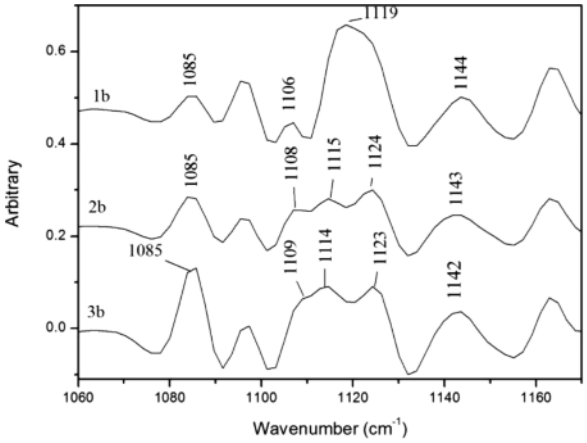

Fig. 9. Second derivative of the C–F symmetric stretching region of neat **6b** (1b), a mixture of **6b** and D_2O (2b) and a mixture of **6b** and H_2O_2 (3b). The derivative curves were multiplied by a factor of 10.

the formation of new spectral features by weak coordination, such as hydrogen bonding between F of the ionic liquid and hydrogen from D_2O or H_2O_2.

NMR spectroscopy

Approximate NMR shifts can be indicated for compounds of a known structure and, *vice versa*, the approximate coordination environment of unknown compounds can be predicted on the basis of chemical shift values [96]. Therefore, ^{11}B, ^{19}F and ^{31}P NMR spectroscopy were performed to show hydrogen bonding in neat **6b** and in the presence of water or hydrogen peroxide. The ^{11}B NMR spectrum of **6b** in deuterated DMSO shows one resonance at −6.58 ppm. After adding water, the resonance is slightly shifted to −6.84 ppm, and upon addition of aqueous H_2O_2 the signal is shifted to –6.75 ppm (see Supporting Information available online; see note at the end of the paper for availability). The ^{19}F NMR spectrum of **6b** shows a signal at –59.55 ppm. When water is added the signal shifts to –61.29 ppm or splits into two signals at −60.64 and –61.23 ppm in the case of adding aqueous H_2O_2 (see Supporting Information). The slight shift of the CF_3 signal points to a change in the chemical environment of the fluorine atoms, pointing to a weak H–F interaction. Noteworthy, the signal splitting is not a consequence of the formation of BF_3 or HF, which would lead to a significantly different peak position. Additionally, the NMR shifts of the cation of **6b** were also studied. While the ^{31}P NMR spectrum of neat **6b** exhibits one resonance at 34.95 ppm, upon addition of water the signal moves to 33.43 ppm. When aqueous H_2O_2 is added the signal of the phosphorus atom is shifted to 33.50 ppm, indicating no significant changes of the chemical environment at the central P atom. Based on the experimental and spectroscopic findings described above, formation of hydrogen bonds between the CF_3 groups of the $[B\{C_6H_3\text{-}3,5\text{-}(CF_3)_2\}_4]^-$ anion of **6b** and hydrogen peroxide lead to the activation of H_2O_2 and to the oxidation of sulfides to sulfoxides.

Conclusion

Ionic compounds containing imidazolium, tetrabutylammonium, tetraalkylphosphonium, and 1,1,3,3-tetramethylguanidium cations associated with $[B(Ar^F)_4]^-$ anions have been synthesized and characterized. The synthesis is facile, and the products are obtained in good yields. All salts exhibit high thermal stability. It is shown that the $[B(C_6H_3\text{-}3,5\text{-}(CF_3)_2)_4]^-$ -containing salts **2b–5b** display lower melting points than the $[B(C_6F_5)_4]^-$ -based salts. The melting points of salts using tetrabutylammonium and 1,1,3,3-tetramethylguanidium as cation are higher than those of any other salts due to the highly symmetric structure. Increasing the size of the ions has a crucial effect on the melting point. Variations of alkyl substituents on the cation can also be used to fine-tune the melting point. In dependence of the structure of the cation, ion pairing *via* hydrogen-fluorine contacts becomes increasingly relevant, which is particularly

the case for 1,3-dialkylimidazolium and guanidinium cations. In the absence of such intramolecular interactions the $[B(Ar^F)_4]^-$ anion can also form H–F bonds with water and hydrogen peroxide, respectively. This leads to an activation of H_2O_2 and can be used to mediate the oxidation of sulfides to sulfoxides.

Experimental Section

General methods

All preparations and manipulation involving air-sensitive materials were performed using standard Schlenk techniques under argon atmosphere. Solvents were dried by standard procedures (Et_2O over Na/benzophenone; CH_2Cl_2 over CaH_2), distilled under argon and kept over 4 Å molecular sieves. All chemicals were purchased from Acros Organics or Aldrich and were of analytical grade. They were used as received. NMR spectra were recorded on a Bruker Avance DPX-400 instrument and referenced to the deuterated solvent in the case of the ^{1}H NMR, C_6F_6 for ^{19}F NMR, $BF_3{\cdot}OEt_2$ for ^{11}B NMR, and H_3PO_4 (85 %) for ^{31}P NMR spectra. IR spectra were recorded on a Varian FTIR-670 spectrometer, using a GladiATR accessory with a diamond ATR element. Elemental analyses were obtained from the microanalytical laboratory at Technische Universität München. Catalytic runs were monitored by GC methods on a Hewlett-Packard instrument HP 5890 Series II equipped with a FID, a Supelco column Alphadex 120 and a Hewlett-Packard integration unit HP 3396 Series II. Thermogravimetry analysis (TGA) was conducted utilizing a Netzsch TG209 system; typically about 10 mg of each sample was heated from 25 to 1000°C at 10 K min^{-1}. Differential scanning analysis (DSC) was performed on a DSCQ2000 instrument (Waters) in a temperature range from −150 to 200°C at 10 K min^{-1}. Melting points were measured by MPM-H2 melting point meters. TLC was performed on silica gel 60F254 plates form E. Merck. Silica gel (0.06 – 0.2 mm 60 Å) was used for column chromatography.

Synthesis of WCCWCAs

General procedures for the synthesis of Li[B(C_6F_5)$_4$], Li[B(C_6H_3-3,5-(CF_3)$_2$)$_4$], Ag[B(C_6F_5)$_4$], and Ag[B(C_6H_3-3,5-(CF_3)$_2$)$_4$]

A 2.5 M solution of *n*-butyl lithium in hexane (17.82 mL) was added slowly to a solution of bromopentafluorobenzene (5 mL, 40 mmol) or 3,5-bis(trifluoromethyl)-5-bromobenzene (7 mL, 40 mmol) in a mixture of diethyl ether (40 mL) at −78°C, and the mixture was stirred for 1 h. This was followed by the dropwise addition of BCl_3 (11.8 mL, 11.8 mmol) dissolved in diethyl ether (20 mL). After 1 h, the resulting suspension was warmed slowly to room temperature. The product Li[B(C_6F_5)$_4$] or Li[B{C_6H_3-3,5-(CF_3)$_2$}$_4$] was separated by filtration, washed with pentane for several times, and then dried under vacuum for one day. Ag[B(C_6F_5)$_4$] and Ag[B(C_6H_3-3,5-(CF_3)$_2$)$_4$] were prepared according to a previously published procedure [72].

*General procedure for the synthesis of **1a–7a***

1 equiv. Li[B(C_6F_5)$_4$] and 1 equiv. [WCC]X were weighed in two different Schlenk tubes and dissolved in CH_2Cl_2. The two solutions were mixed and stirred for 2 h at room temperature, and then filtered. The solvent was removed under high vacuum for 4 h. The product was washed three times with dry *n*-hexane and then dried under vacuum for one day.

*Improved procedure for the synthesis of **1a–7a***

To a mixture of equimolar amounts of Ag[B(C_6F_5)$_4$] and [WCC]X dry CH_2Cl_2 (20 mL) was added. The mixture was stirred under exclusion of light at room temperature for 10 min. The precipitate was removed by filtration, and the filtrate was dried for 4 h under high vacuum. The product was washed several times with *n*-hexane and dried under vacuum for one day.

*Experimental data for **1a**:* Ag[B(C_6F_5)$_4$] (0.787 g, 1 mmol), [Bmim]Br (0.218 g, 1 mmol); isolated yield: 0.73 g (89 %). – ^{1}H NMR ([D$_6$]DMSO, 400 MHz, r. t., ppm): $\delta = 0.89$ (t, 3H), 1.25 (m, 2H), 1.76 (m, 2H), 3.85 (s, 3H), 4.16 (t, 2H), 7.71 (m, 1H), 7.77 (m, 1H), 9.12 (s, 1H). – ^{19}F NMR ([D$_6$]DMSO, 377 MHz, r. t., ppm): $\delta = -131.26$ (s, 8F), −161.66 (t, 4F), −165.60 (t, 8F). – ^{11}B NMR ([D$_6$]DMSO, 128 MHz, r. t., ppm): $\delta = -16.7$ (s). – IR (cm^{-1}): $\nu = 480$(w), 573 (w), 660 (m), 683 (m), 739 (m), 772 (m), 974 (vs), 1082 (vs), 1272 (m), 1373 (w), 1486 (vs), 1513 (s), 1642 (m), 1953 (w), 2159 (w), 2545 (vw). – Elemental analysis for $C_{32}H_{14}N_2BF_{20}$ (%): calcd. C 46.91, H 1.97, N 3.42; found C 46.25, H 2.10, N 3.87.

*Experimental data for **2a**:* Ag[B(C_6F_5)$_4$] (0.787 g, 1 mmol), [Bdmim]Br (0.223 g, 1 mmol); isolated yield: 0.76 g (92 %). – ^{1}H NMR ([D$_6$]DMSO, 400 MHz, r. t., ppm): $\delta = 0.89$ (t, 3H), 1.27 (m, 2H), 1.68 (m, 2H), 2.58 (s, 3H), 3.75 (s, 3H), 4.11 (t, 2H), 7.61 (m, 1H), 7.64 (m, 1H). – ^{19}F NMR ([D$_6$]DMSO, 377 MHz, r. t., ppm): $\delta = -132.42$ (s, 8F), −161.54 (t, 4F), −166.02 (t, 8F). – ^{11}B NMR ([D$_6$]DMSO, 128 MHz, r. t., ppm): $\delta = -16.8$ (s). – IR (cm^{-1}): $\nu = 477$ (vw), 573 (w), 621 (w), 659 (m), 683 (w), 830 (m), 957 (vs), 1081 (s), 1163 (m), 1274 (m), 1374 (w), 1458 (vs), 1512 (s), 1567 (w), 1592 (w), 1642 (m), 1957 (m), 2158 (m), 2547

(w). – Elemental analysis for $C_{33}H_{17}N_2BF_{20}$ (%): calcd. C 47.56, H 2.18, N 3.36; found C 46.63, H 2.48, N 3.89.

Experimental data for ***3a****:* Ag[B(C_6F_5)$_4$] (0.787 g, 1 mmol), [C_{12}mim]Br (0.331 g, 1 mmol); isolated yield: 0.87 g (93 %). – ^{1}H NMR ([D$_6$]DMSO, 400 MHz, r. t., ppm): $\delta = 0.78$ (t, 3H), 1.20 (m, 18H), 1.75 (m, 2H), 3.83 (3H), 4.13(t, 2H), 7.68 (s, 1H), 7.73 (s, 1H), 9.09 (s, 1H). – ^{19}F NMR ([D$_6$]DMSO, 377 MHz, r. t., ppm): $\delta = -130.28$(s, 8F), −159.55 (t, 4F), −164.01 (t, 8F). – ^{11}B NMR ([D$_6$]DMSO, 128 MHz, r. t., ppm): $\delta = -16.51$ (s). – IR (cm^{-1}): $\nu = 475$ (vw), 573 (m), 610 (w), 623 (m), 660 (s), 682 (m),734 (w), 756 (m), 773 (m), 800 (vw), 831 (w), 976 (vs), 1080 (vs), 1165 (m), 1274 (m), 1461 (vs), 1514 (s), 1563 (w), 1589 (w), 1644 (m), 2856 (w), 2927 (w). – Elemental analysis for $C_{40}H_{32}N_2BF_{20}$ (%): calcd. C 51.58, H 3.46, N 3.01; found C 51.39, H 3.63, N 3.16.

Experimental data for ***4a****:* Ag[B(C_6F_5)$_4$] (0.787 g, 1 mmol), [NBu_4]Br (0.322 g, 1 mmol); isolated yield: 0.86 g (93 %). – ^{1}H NMR ($CDCl_3$, 400 MHz, r. t., ppm): $\delta = 0.97$ (t, 12H), 1.25 (m, 8H), 1.53 (m, 8H), 3.05 (m, 8H). – ^{19}F NMR ([D$_6$]DMSO, 377 MHz, r. t., ppm): $\delta = -131.08$ (s, 8F), −160.51 (t, 4F), −161.40 (t, 8F). – ^{11}B NMR ([D$_6$]DMSO, 128 MHz, r. t., ppm): $\delta = -16.37$ (s). – IR (cm^{-1}): $\nu = 476$ (w), 574 (w), 660 (m), 682 (m), 773 (w), 977 (vs), 1085 (s), 1272 (m), 1461 (vs), 1513 (s), 1643 (w), 1960 (w), 2169 (w), 2878 (w), 2963 (w). – Elemental analysis for $C_{40}H_{36}BF_{20}N$ (%): calcd. C 52.14, H 3.94, N 1.52; found C 51.07, H 4.10, N 1.66.

Experimental data for ***5a****:* Ag[B(C_6F_5)$_4$] (0.787 g, 1 mmol), [PBu_4]Br (0.338 g, 1 mmol); isolated yield: 0.82 g (87 %). – ^{1}H NMR ([D$_6$]DMSO, 400 MHz, r. t., ppm): $\delta = 0.86$ (m, 12H), 1.38 (m, 16H), 2.14 (m, 8H). – ^{19}F NMR ([D$_6$]DMSO, 377 MHz, r. t., ppm): $\delta = -130.20$(s, 8F), −159.07 (t, 4F), −163.72(t, 8F). – ^{11}B NMR ([D$_6$]DMSO, 128 MHz, r. t., ppm): $\delta = -16.47$ (s). – ^{31}P NMR ([D$_6$]DMSO, 162 MHz, r. t., ppm): $\delta = 29.74$ (s). – IR (cm^{-1}): $\nu = 574$ (w), 660 (m), 683 (w), 755 (m), 772 (m), 906 (m), 975 (vs), 1082 (vs), 1273 (w), 1382 (vw), 1459 (vs), 1512 (s), 1642 (m), 1958 (vw), 2159 (vw), 2873 (w), 2932 (w), 2960 (w). – Elemental analysis for $C_{40}H_{36}BF_{20}P$ (%): calcd. C 51.19, H 3.87; found C 50.27, H 4.03.

Experimental data for ***6a****:* Ag[B(C_6F_5)$_4$] (0.787 g, 1 mmol), [$P_{4,4,4,14}$]Cl (0.434 g, 1 mmol); isolated yield: 0.92 g (85 %). – ^{1}H NMR ([D$_6$]DMSO, 400 MHz, r. t., ppm): $\delta = 078$ (t, 3H), 0.88 (t, 9H), 1.21 (m, 20H), 1.43 (m, 16H), 2.17 (m, 8H). – ^{19}F NMR ([D$_6$]DMSO, 377 MHz, r. t., ppm): $\delta = -130.23$ (s, 8F), −160.21 (t, 4F), −164.35 (t, 8F,). – ^{11}B NMR ([D$_6$]DMSO, 128 MHz, r. t., ppm): $\delta = -16.51$ (s). – ^{31}P NMR ([D$_6$]DMSO, 162 MHz, r. t., ppm): $\delta = 33.77$ (s). – IR (cm^{-1}): $\nu = 475$ (vw), 573 (w), 602 (w), 610 (w), 660 (m), 683 (w), 726 (vw), 755 (m), 774 (vs), 909 (vw), 977 (vs), 1083 (vs), 1274 (m), 1373 (vw), 1461 (vs), 1512 (s), 1642 (m), 2857 (w), 2929 (w). – Elemental analysis for $C_{50}H_{56}BF_{20}P$ (%): calcd. C 55.67, H 5.23; found C 55.66, H 5.96.

Experimental data for ***7a****:* Ag[B(C_6F_5)$_4$] (0.787 g, 1 mmol), [TMG]Cl (0.151 g, 1 mmol); isolated yield: 0.75 g (94 %). – ^{1}H NMR ([D$_6$]DMSO, 400 MHz, r. t., ppm): $\delta = 1.89$ (s, 12H), 7.89 (s, 2H). – ^{19}F NMR ([D$_6$]DMSO, 377 MHz, r. t., ppm): $\delta = -130.32$ (s, 8F), −159.30 (t, 4F), −163.91 (t, 8F). – ^{11}B NMR ([D$_6$]DMSO, 128 MHz, r. t., ppm): $\delta = -16.49$ (s). – IR (cm^{-1}): $\nu = 440$ (w), 661 (s), 756 (w), 774 (m), 976 (vs), 1080 (s), 1276 (m), 1460 (vs), 1511 (s), 1628 (s), 1958 (w), 2158 (w), 3433 (vw). – Elemental analysis for $C_{29}H_{14}N_3BF_{20}$ (%): calcd. C 43.80, H 1.77, N 5.28; found C 43.52, H 1.86, N 5.38.

General procedure for the synthesis of ***1b–7b***

In a Schlenk flask, to a mixture of equimolar amounts of Ag[B(C_6H_3-3,5-(CF_3)$_2$)$_4$] and [WCC]X dry CH_2Cl_2 (20 mL) was added. The mixture was stirred under exclusion of light at room temperature for 10 min. The precipitate was removed by filtration, and the filtrate was dried in high vacuum for 4 h. The product was washed several times with *n*-hexane and dried under vacuum for one day.

Experimental data for ***1b****:* Ag[B{C_6H_3-3,5-(CF_3)$_2$}$_4$] (0.971 g, 1 mmol), [C_4mim]Br (0.218 g , 1 mmol); isolated yield: 0.95 g (95 %). – ^{1}H NMR ([D$_6$]DMSO, 400 MHz, r. t., ppm): $\delta = 0.89$ (t, 3H), 1.26 (m, 2H), 1.75 (m, 2H), 3.84 (s, 3H), 4.15 (t, 2H), 7.62 (m, 8H), 7.70 (m, 4H), 7.73 (m, 1H), 7.71 (m, 1H), 9.11 (s, 1H). – ^{19}F NMR ([D$_6$]DMSO, 377 MHz, r. t., ppm): $\delta = -59.96$ (s, 6F). – ^{11}B NMR ([D$_6$]DMSO, 128 MHz, r. t., ppm): $\delta = -6.58$ (s). – IR (cm^{-1}): $\nu = 448$ (w), 621 (m), 669 (s), 712 (s), 743 (m), 837 (m), 887 (m), 1109 (vs), 1272 (vs), 1353 (s), 1568 (vw), 1608 (vw), 2961 (vw). – Elemental analysis for $C_{40}H_{28}N_2BF_{24}$ (%): calcd. C 47.88, H 2.81, N 2.79; found C 47.54, H 2.84, N 3.08.

Experimental data for ***2b****:* Ag[B{C_6H_3-3,5-(CF_3)$_2$}$_4$] (0.971 g, 1 mmol), [Bdmin]Br (0.223 g, 1 mmol); isolated yield: 0.97 g (95 %). – ^{1}H NMR ([D$_6$]DMSO, 400 MHz, r. t., ppm): $\delta = 0.87$ (t, 3H), 1.25 (m, 2H), 1.64 (m, 2H), 2.48 (s, 3H), 3.73 (s, 3H), 4.08 (t, 2H), 7.61 (m, 12H), 7.62 (m, 2H). – ^{19}F NMR ([D$_6$]DMSO, 377 MHz, r. t., ppm): $\delta = -59.55$ (s, 6F). – ^{11}B NMR ([D$_6$]DMSO, 128 MHz, r. t., ppm): $\delta = -6.59$ (s). – IR (cm^{-1}): $\nu = 669$ (vs), 715 (s), 742 (m), 838 (m), 889 (s), 1115 (vs), 1274 (vs), 1352 (s), 1462

(w), 1535 (vw), 2193 (w), 2959 (vw). – Elemental analysis for $C_{41}H_{30}N_2BF_{24}$ (%): calcd. C48.40, H 2.97, N 2.75; found C 47.70, H 2.96, N 3.03.

Experimental data for ***3b****:* Ag[B{C_6H_3-3,5-$(CF_3)_2$}$_4$] (0.971 g, 1 mmol), [C_{12}mim]Br (0.331 g, 1 mmol); isolated yield: 1.03 g (93 %). – ^{1}H NMR ([D$_6$]DMSO, 400 MHz, r. t., ppm): $\delta = 0.72$ (t, 3H), 1.16 (m, 18H), 1.75 (m, 2H), 3.84 (3H), 4.13(t, 2H), 7.69 (m, 12H), 7.74 (s, 1H), 7.75 (s, 1H), 9.11 (s, 1H). – ^{19}F NMR ([D$_6$]DMSO, 377 MHz, r. t., ppm): $\delta = -60.03$ (s, 6F). – ^{11}B NMR ([D$_6$]DMSO, 128 MHz, r. t., ppm): $\delta = -6.54$(s). – IR (cm^{-1}): $\nu = 446$ (m), 580 (vw), 622 (w), 667 (s), 682 (m), 707(m), 715(m), 742 (w), 838(m), 888 (s), 899 (m), 949 (vw), 1114 (vs), 1158 (vs), 1272 (vs), 1353 (vs), 1466 (vw), 1570 (vw), 1610 (vw), 2860 (w), 2934 (w). – Elemental analysis for $C_{48}H_{44}N_2BF_{24}$ (%): calcd. C 51.68, H 3.98, N 2.51; found C 51.81, H 3.90, N 2.52.

Experimental data for ***4b****:* Ag[B{C_6H_3-3,5-$(CF_3)_2$}$_4$] (0.971 g, 1 mmol), [NBu_4]Br (0.322 g, 1 mmol); isolated yield: 1.04 g (94 %). – ^{1}H NMR ([D$_6$]DMSO, 400 MHz, r. t., ppm): $\delta = 0.88$ (t, 12H), 1.27 (m, 8H), 1.55 (m, 8H), 3.15 (m, 8H), 7.58 (m, 12H). – ^{19}F NMR ([D$_6$]DMSO, 377 MHz, r. t., ppm): $\delta = -59.87$ (s, 6F). – ^{11}B NMR ([D$_6$]DMSO, 128 MHz, r. t., ppm): $\delta = -6.81$ (s). – IR (cm^{-1}): $\nu = 450$ (vw), 670 (s), 712 (s), 799 (m), 838 (m), 889 (m), 1117 (vs), 1271 (vs), 1353 (s), 1470 (w), 1608 (vw), 2179 (w), 2964 (w). – Elemental analysis for $C_{48}H_{48}NBF_{24}$ (%): calcd. C 52.14, H 4.38, N 1.27; found C 51.81, H 4.70, N 1.44.

Experimental data for ***5b****:* Ag[B{C_6H_3-3,5-$(CF_3)_2$}$_4$] (0.971 g, 1 mmol), [PBu_4]Br (0.338 g, 1 mmol); isolated yield: 1.02 g (91 %). – ^{1}H NMR ([D$_6$]DMSO, 400 MHz, r. t., ppm): $\delta = 0.82$ (m, 12H), 1.36 (m, 16H), 2.10 (m, 8H); 7.57 (m, 12H). – ^{19}F NMR ([D$_6$]DMSO, 377 MHz, r. t., ppm): $\delta = -59.66$ (s, 6F). – ^{11}B NMR ([D$_6$]DMSO, 128 MHz, r. t., ppm): $\delta = -6.59$ (s). – ^{31}P NMR ([D$_6$]DMSO, 162 MHz, r. t., ppm): $\delta = 33.76$ (s). – IR (cm^{-1}): $\nu = 447$ (vw), 667 (m), 712 (m), 837 (w), 886 (m), 1114 (vs), 1272 (vs), 1353 (s), 1465 (w), 1610 (vw), 2542 (vw), 2875 (vw), 2963 (vw). – Elemental analysis for $C_{48}H_{48}BF_{20}P$ (%): calcd. C 51.35, H 4.31; found: C 51.07, H 4.46.

Experimental data for ***6b****:* Ag[B{C_6H_3-3,5-$(CF_3)_2$}$_4$] (0.971 g, 1 mmol), [$P_{4,4,4,14}$]Cl (0.434 g, 1 mmol); isolated yield: 1.15 g (91 %). – ^{1}H NMR ([D$_6$]DMSO, 400 MHz, r. t., ppm): $\delta = 0.73$ (t, 3H), 0.84 (t, 9H), 1.16 (m, 20H), 1.40 (m, 16H), 2.13 (m, 8H), 7.57 (m, 12H). – ^{19}F NMR ([D$_6$]DMSO, 377 MHz, r. t., ppm): $\delta = -59.55$ (s, 6F). – ^{11}B NMR ([D$_6$]DMSO, 128 MHz, r. t., ppm): $\delta = -6.58$ (s). – ^{31}P NMR ([D$_6$]DMSO, 162 MHz, r. t., ppm): $\delta = 33.54$ (s). – IR (cm^{-1}): $\nu = 403$ (w), 450 (w), 618 (vw), 669 (s), 681 (m), 710 (s), 744 (vw), 838 (m), 887 (m), 934 (vw), 1001 (vw), 1112 (vs), 1161 (vs), 1274 (vs), 1351 (s), 1468 (w), 1608 (w), 2858 (w), 2927 (w). – Elemental analysis for $C_{58}H_{68}BF_{24}P$ (%): calcd. C 55.16, H 5.43; found C 55.79, H 5.81.

Experimental data for ***7b****:* Ag[B{C_6H_3-3,5-$(CF_3)_2$}$_4$] (0.971 g, 1 mmol), [TMG]Cl (0.151 g, 1 mmol); isolated yield: 0.93 g (95 %). – ^{1}H NMR ([D$_6$]DMSO, 400 MHz, r. t., ppm): $\delta = 2.86$ (s, 12H), 7.66 (m, 12H), 7.80 (s, 2H). – ^{19}F NMR ([D$_6$]DMSO, 377 MHz, r. t., ppm): $\delta = -60.02$ (s, 6F). – ^{11}B NMR ([D$_6$]DMSO, 128 MHz, r. t., ppm): $\delta = -6.58$ (s). – IR (cm^{-1}): $\nu = 449$ (w), 669 (m), 709 (m), 837 (w), 885 (m), 1109 (vs), 1274 (vs), 1353 (s), 1415 (w), 1635 (m), 2210 (w), 2548 (vw). – Elemental analysis for $C_{37}H_{26}N_3BF_{24}$ (%): calcd. C 45.37, H 2.68, N 4.29; found C 45.20, H 2.72, N 4.35.

Oxidation of sulfides to sulfoxides mediated by WCCWCA ***6b***

Typical procedure for the oxidation of the sulfides in [$P_{4,4,4,14}$][B{C_6H_3-3,5-$(CF_3)_2$}$_4$]: To a stirred solution of the sulfide (2 mmol, 0.24 mL) in **6b** (0.50 mL), an aqueous solution of hydrogen peroxide (30 % in water) (0.51 mL, 5 mmol) was added in 2 to 3 portions at room temperature. The progress of the reaction was followed by TLC. The reaction mixture was extracted with *n*-hexane-diethyl ether 2:1 v/v (5 × 5 mL), and the extract was dried over anhydrous $MgSO_4$. The crude product was obtained by rolling evaporation and purified by column chromatography separation (silica gel using *n*-hexane-ethyl acetate 90:10 v/v). The yield and selectivity of methyl phenyl sulfoxide in kinetic and recycle experiments was calculated from calibration curves ($r^2 > 0.999$) recorded using 3-methylanisole and 1,4-diacetylbenzene as internal standard. The WCCWCA was extracted with CH_2Cl_2 and then treated with MnO_2 to destroy the excess peroxide. The obtained liquid was dried over anhydrous $MgSO_4$ and then dried for 4 h *in vacuo* at 50°C to remove CH_2Cl_2. Fresh substrate and hydrogen peroxide were then added for a new reaction cycle. All products were characterized by melting point, ^{1}H NMR, ^{13}C NMR and IR spectroscopy (see the Supporting Information).

Single-crystal X-ray structure determinations

Data were collected on an X-ray single-crystal diffractometer equipped with a CCD detector (Bruker APEX II, κ-CCD), a rotating anode (Bruker AXS, FR591) with MoK_α radiation ($\lambda = 0.71073$ Å), and a graphite monochromator by using the SMART software package [105]. The measurements were performed on a single crystal coated with perfluorinated ether. The crystal was fixed on the top of a glass fiber and transferred to the diffractometer. The crystal was frozen in a stream of cold nitrogen. A matrix scan was used to deter-

mine the initial lattice parameters. Reflections were merged and corrected for Lorenz and polarization effects, scan speed, and background using SAINT [73]. Absorption corrections, including odd and even ordered spherical harmonics were performed using SADABS [106]. Space group assignments were based upon systematic absences, *E* statistics, and successful refinement of the structures. The structures were solved by Direct Methods with the aid of successive difference Fourier maps and were refined against all data using WINGX [107] based on SIR92 [108]. If not mentioned otherwise, non-hydrogen atoms were refined with anisotropic displacement parameters. Methyl hydrogen atoms were refined as part of rigid rotating groups, with C–H = 0.98 Å and $U_{iso}(H) = 1.5 \cdot U_{eq}(C)$. Other H atoms were placed in calculated positions and refined using a riding model, with methylene and aromatic C–H distances of 0.99 and 0.95 Å, respectively, and $U_{iso}(H) = 1.2 \cdot U_{eq}(C)$. Full-matrix least-squares refinements were carried out by minimizing $\Sigma w(F_o^2 - F_c^2)^2$ with the SHELXL-97 weighting scheme [109]. Neutral atom scattering factors for all atoms and anomalous dispersion corrections for the non-hydrogen atoms were taken from International Tables for Crystallography [110]. Images of the crystal structures were generated by PLATON [111].

CCDC 956714 (**2b**), 956711 (**5a**), 956712 (**6b**), and 956713 (**7a**) contain the supplementary crystallographic data for this compound. These data can be obtained free of charge from The Cambridge Crystallographic Data Centre *via* www.ccdc.cam.ac.uk/data_request/cif.

*Single-crystal X-ray structure determination of compound **2b***

Crystal data: empirical formula: $C_{41}H_{29}BF_{24}N_2$; $M_r = 1016.47$; crystal color and shape: colorless block, crystal dimensions: $0.38 \times 0.51 \times 0.51$ mm^3; crystal system: monoclinic; space group: $P2_1/c$ (no. 14); $a = 20.1391(5)$, $b = 13.9355(3)$, $c = 16.2559(4)$ Å, $\beta = 111.2143(9)°$, $V = 4253.03(18)$ Å^3, $Z = 4$, $\lambda(\text{MoK}\alpha) = 0.71073$ Å, $\mu = 0.2$ mm^{-1}, $\rho_{calcd.} = 1.59$ g cm^{-3}, $T = 123(1)$ K, $F(000) = 2040\,e$; θ-range = 1.82 – 25.50°; data collected: 133524; independent data [$I_o > 2\,\sigma(I_o)$ / all data / R_{int}]: 6806 / 7872 / 0.019; data/restraints / parameters: 7872 / 0 / 785; R_1 [$I_o > 2\,\sigma(I_o)$ / all data]: 0.0396 / 0.0472; *wR*2 [$I_o > 2\,\sigma(I_o)$ / all data]: 0.0937 / 0.1006; GOF = 1.020; $\Delta\rho_{max/min}$: 0.47 / −0.43 e Å^{-3}.

*Single-crystal X-ray structure determination of compound **5a***

Crystal data: empirical formula: $C_{40}H_{36}BF_{20}P$; $M_r = 938.47$; crystal color and shape: colorless fragment, crystal dimensions: $0.48 \times 0.56 \times 0.61$ mm^3; crystal system: orthorhombic; space group: $Pca2_1$ (no. 29); $a = 18.9591(7)$, $b = 22.2987(8)$, $c = 19.2449(7)$ Å, $V = 8136.0(5)$ Å^3, $Z = 8$, $\lambda(\text{MoK}\alpha) = 0.71073$ Å, $\mu = 0.2$ mm^{-1}, $\rho_{calcd.} = 1.53$ g cm^{-3}, $T = 123(1)$ K, $F(000) = 3808\,e$; θ-range = 0.91 – 25.40°; data collected: 231060; independent data [$I_o > 2\,\sigma(I_o)$ / all data / R_{int}]: 14524 / 14933 / 0.036; data/restraints / parameters: 14933 / 1 / 1126; R_1 [$I_o > 2\,\sigma(I_o)$ / all data]: 0.0245 / 0.0257; *wR*2 [$I_o > 2\,\sigma(I_o)$ / all data]: 0.0667 / 0.0682; GOF = 1.046; $\Delta\rho_{max/min}$: 0.27 / −0.22 e Å^{-3}.

*Single-crystal X-ray structure determination on compound **6b***

Crystal data: empirical formula: $C_{58}H_{68}BF_{24}P$; $M_r = 1262.90$; crystal color and shape: colorless fragment, crystal dimensions: $0.56 \times 0.59 \times 0.59$ mm^3; crystal system: triclinic; space group: $P\bar{1}$ (no. 2); $a = 12.9732(4)$, $b = 14.0401(4)$, $c = 18.0389(5)$ Å, $\alpha = 105.4144(14)°$, $\beta = 97.8526(13)°$, $\gamma = 97.5892(13)°$, $V = 3088.64(16)$ Å^3, $Z = 2$, $\lambda(\text{MoK}\alpha) = 0.71073$ Å, $\mu = 0.2$ mm^{-1}, $\rho_{calcd.} = 1.36$ g cm^{-3}, $T = 123(1)$ K, $F(000) = 1304\,e$; θ-range = 1.19 – 25.43°; data collected: 95414; independent data [$I_o > 2\,\sigma$ (I_o) / all data / R_{int}]: 10444 / 11372 / 0.030; data/restraints / parameters: 11372 / 0 / 845; R_1 [$I_o > 2\sigma$ (I_o) / all data]: 0.0363 / 0.0399; *wR*2 [$I_o > 2\,\sigma(I_o)$ / all data]: 0.0889 / 0.0929; GOF = 1.015; $\Delta\rho_{max/min}$: 0.53 / −0.50 e Å^{-3}.

*Single-crystal X-ray structure determination of compound **7a***

Crystal data: empirical formula: $C_{29}H_{14}BF_{20}N_3$; $M_r = 795.24$; crystal color and shape: colorless fragment, crystal dimensions: $0.10 \times 0.25 \times 0.36$ mm^3; crystal system: triclinic; space group: $P\bar{1}$ (no. 2); $a = 8.1571(2)$, $b = 12.7109(4)$, $c = 14.5597(4)$ Å, $\alpha = 89.4091(12)°$, $\beta = 83.9006(12)°$, $\gamma = 81.7908(12)°$, $V = 1485.66(7)$ Å^3, $Z = 2$, $\lambda(\text{MoK}\alpha) = 0.71073$ Å, $\mu = 0.2$ mm^{-1}, $\rho_{calcd.} = 1.78$ g cm^{-3}, $T = 123(1)$ K, $F(000) = 788\,e$; θ-range = 1.41 – 25.43°; data collected: 51233; independent data [$I_o > 2\,\sigma(I_o)$ / all data / R_{int}]: 5014 / 5423 / 0.039; data/restraints / parameters: 5423 / 0 / 534; R_1 [$I_o > 2\,\sigma(I_o)$ / all data]: 0.0296 / 0.0322; *wR*2 [$I_o > 2\,\sigma(I_o)$ / all data]: 0.0778 / 0.0808; GOF = 1.031; $\Delta\rho_{max/min}$: 0.29 / −0.19 e Å^{-3}.

Supporting information

Detailed information on all crystal structure determinations, spectroscopic data, and characterization of all sulfoxides are given as Supporting Information (17 pages) available online (DOI: 10.5560/ZNB.2014-4165).

Acknowledgement

B. Z. and. S. L. thank the TUM Graduate School for financial support. S.-L. Z. thanks the National Science Foundation of China (21071073) and the Cooperation Project (21111130584) for financial support.

[1] T. Welton, *Chem. Rev.* **1999**, *99*, 2071 – 2083.
[2] T. Welton, *Coord. Chem. Rev.* **2004**, *248*, 2459 – 2477.
[3] J. P. Hallett, T. Welton, *Chem. Rev.* **2011**, *111*, 3508 – 3576.
[4] P. Wasserscheid, W. Keim, *Angew. Chem. Int. Ed.* **2000**, *39*, 3772 – 3789.
[5] R. Sheldon, *Chem. Commun.* **2001**, 2399 – 2407.
[6] J. Dupont, R. F. de Souza, P. A. Z. Suarez, *Chem. Rev.* **2002**, *102*, 3667 – 3692.
[7] N. V. Plechkova, K. R. Seddon, *Chem. Soc. Rev.* **2008**, *37*, 123 – 150.
[8] R. Noyori, M. Aoki, K. Sato, *Chem. Commun.* **2003**, 1977 – 1986.
[9] V. I. Pârvulescu, C. Hardacre, *Chem. Rev.* **2007**, *107*, 2615 – 2665.
[10] T. L. Greaves, C. J. Drummond, *Chem. Rev.* **2008**, *108*, 206 – 237.
[11] M. A. P. Martins, C. P. Frizzo, D. N. Moreira, N. Zanatta, H. G. Bonacorso, *Chem. Rev.* **2007**, *107*, 2592 – 2614.
[12] R. Giernoth, *Angew. Chem. Int. Ed.* **2010**, *49*, 2834 – 2849.
[13] S. G. Lee, *Chem. Commun.* **2006**, 1049 – 1063.
[14] J. T. Tindale, K. D. Hartlen, A. Alizadeh, M. S. Workentin, P. J. Ragogna, *Chem. Eur. J.* **2010**, *16*, 9068 – 9075.
[15] A. Ouadi, B. Gadenne, P. Hesemann, J. J. E. Moreau, I. Billard, C. Gaillard, S. Mekki, G. Moutiers, *Chem. Eur. J.* **2006**, *12*, 3704 – 3081.
[16] T. Inagaki, T. Mochida, M. Takahashi, C. Kanadan, T. Saito, D. Kawahara, *Chem. Eur. J.* **2012**, *18*, 6795 – 6804.
[17] Z. R. Fei, T. J. Geldbach, D. B. Zhao, P. J. Dyson, *Chem. Eur. J.* **2006**, *8*, 156 – 160.
[18] D. Betz, P. Altmann, M. Cokoja, W. A. Herrmann, F. E. Kühn, *Coord. Chem. Rev.* **2011**, *255*, 1518 – 1540.
[19] L. Graser, D. Betz, M. Cokoja, F. E. Kühn, *Curr. Inorg. Chem.* **2011**, *1*, 166 – 181.
[20] I. Krossing, J. M. Slattery, C. Daguenet, P. J. Dyson, A. Oleinikova, H. Weingärtner, *J. Am. Chem. Soc.* **2006**, *128*, 13427 – 13434.
[21] P. Hapiot, C. Lagrost, *Chem. Rev.* **2008**, *108*, 2238 – 2264.
[22] I. J. B. Lin, C. S. Vasam, *J. Organomet. Chem.* **2005**, *690*, 3498 – 3512.
[23] Q. Zhang, S. Zhang, Y. Deng, *Green Chem.* **2011**, *13*, 2619 – 2637.
[24] U. Preiss, J. M. Slattery, I. Krossing, *Ind. Eng. Chem. Res.* **2009**, *48*, 2290 – 2296.
[25] J. M. Slattery, C. Daguenet, P. J. Dyson, T. J. S. Schubert, I. Krossing, *Angew. Chem. Int. Ed.* **2007**, *46*, 5384 – 5388.
[26] I. Krossing, I. Raabe, *Angew. Chem. Int. Ed.* **2004**, *43*, 2066 – 2090.
[27] K. Dong, S. Zhang, *Chem. Eur. J.* **2012**, *18*, 2748 – 2761.
[28] A. R. Choudhury, N. Winterton, A. Steiner, A. I. Cooper, K. A. Johnson, *J. Am. Chem. Soc.* **2005**, *127*, 16792 – 16793.
[29] A. R. Choudhury, T. N. G. Row, *CrystEngComm* **2006**, *8*, 265 – 274.
[30] W. M. Reichert, J. D. Holbery, R. P. Swatloski, K. E. Gutowski, A. E. Visser, M. Nieuwenhuyzen, K. R. Seddon, R. D. Rogers, *Cryst. Growth Des.* **2007**, *7*, 1106 – 1114.
[31] J. D. Holbrey, W. M. Reichert, R. D. Rogers, *Dalton Trans.* **2004**, 2267 – 2271.
[32] K. Fumino, A. Wulf, R. Ludwig, *Angew. Chem. Int. Ed.* **2008**, *47*, 3830 – 3834.
[33] R. P. Swatloski, J. D. Holbrey, R. D. Rogers, *Green Chem.* **2003**, *5*, 361 – 363.
[34] C. Roth, T. Peppel. K. Fumino, M. Köckerling, R. Ludwig, *Angew. Chem. Int. Ed.* **2010**, *49*, 10221 – 10224.
[35] S. H. Strauss, *Chem. Rev.* **1993**, *93*, 927 – 942.
[36] C. A. Reed, *Acc. Chem. Res.* **1998**, *31*, 133 – 139.
[37] A. Bösmann, G. Francio, E. Janssen, W. Leitner, P. Wasserscheid, *Angew. Chem. Int. Ed.* **2001**, *40*, 2697 – 2699.
[38] A. Reisinger, I. Krossing, *Coord. Chem. Rev.* **2006**, *250*, 2721 – 2744.
[39] I. Raabe, K. Wagner, K. Guttsche, M. Wang, M. Grätzel, G. S. Quiñones, I. Krossing, *Chem. Eur. J.* **2009**, *15*, 1966 – 1976.
[40] T. Timofte, S. Pitula, A. V. Mudring, *Inorg. Chem.* **2007**, *46*, 10938 – 10940.
[41] Z. B. Zhou, H. Matsumoto, K. Tatsumi, *Chem. Eur. J.* **2004**, *10*, 6581 – 6591.
[42] Z. B. Zhou, H. Matsumoto, K. Tatsumi, *Chem. Eur. J.* **2005**, *11*, 752 – 766.
[43] H. Matsumoto, Z. B. Zhou, H. Sakaebe, K. Tatsami, *Electrochemistry* **2005**, *73*, 633 – 635.

[44] Z. B. Zhou, H. Matsumoto, K. Tatsumi, *ChemPhys Chem* **2005**, *6*, 1324 – 1332.
[45] A. S. Larsen, J. D. Holbrey, F. S. Tham, C. A. Reed, *J. Am. Chem. Soc.* **2000**, *122*, 7264 – 7272.
[46] J. Dymon, R. Wibby, J. Kleingardner, J. M. Tanski, I. A. Guzei, J. D. Holbrey, A. S. Larsen, *Dalton Trans.* **2008**, 2999 – 3006.
[47] M. Bürchner, A. M. T. Erle, H. Scherer, I. Krossing, *Chem. Eur. J.* **2012**, *18*, 2254 – 2262.
[48] A. R. Katritzkhy, S. Singh, K. Kirichenko, M. Smiglak, J. D. Holbrey, W. M. Reichert, S. K. Spear, R. D. Rogers, *Chem. Eur. J.* **2006**, *12*, 4630 – 4641.
[49] M. Smiglak, C. C. Hines, T. B. Wilson, S. Singh, A. S. Vincek, K. Kirichenko, A. R. Katritzky, R. D. Rogers, *Chem. Eur. J.* **2011**, *16*, 1572 – 1584.
[50] M. Finze, E. Bernhardt, H. Willner, *Angew. Chem. Int. Ed.* **2007**, *46*, 9180 – 9196.
[51] P. Jutzi, C. Müller, A. Stammler, H.-G. Stammler, *Organometallics* **2000**, *19*, 1442 – 1444.
[52] C. A. Reed, *Acc. Chem. Res.* **1998**, *31*, 325 – 332.
[53] R. E. LaPointe, G. P. Roof, K. A. Abbound, J. Klosin, *J. Am. Chem. Soc.* **2000**, *122*, 9560 – 9561.
[54] S. J. Lancaster, D. A. Walker, M. Thornton-Pett, M. Bochmann, *Chem. Commun.* **1999**, 1533 – 1534.
[55] E. Y.-X. Chen, T. J. Marks, *Chem. Rev.* **2000**, *100*, 1391 – 1434.
[56] S. D. Ittel, L. K. Johnson, M. Brookhart, *Chem. Rev.* **2000**, *100*, 1169 – 1203.
[57] S. F. Rach, F. E. Kühn, *Chem. Rev.* **2009**, *109*, 2061 – 2080.
[58] Y. Li, M. Cokoja, F. E. Kühn, *Coord. Chem. Rev.* **2011**, *255*, 1541 – 1557.
[59] I. I. E. Markovits, W. A. Eger, S. Yue, M. Cokoja, C. J. Münchmeyer, B. Zhang, M.-D. Zhou, A. Genest, J. Mink, S.-L. Zang, N. Rösch, F. E. Kühn, *Chem. Eur. J.* **2013**, *19*, 5972 – 5979.
[60] B. Zhang, S. Li, S. Yue, M. Cokoja, M.-D. Zhou, S.-L. Zang, F. E. Kühn, *J. Organomet. Chem.* **2013**, *744*, 108 – 112.
[61] B. Zhang, S. Li, A. Pöthig, M. Cokoja, S.-L. Zang, W. A. Herrmann, F. E. Kühn, *Z. Naturforsch.* **2013**, *68b*, 587 – 597.
[62] L. R. Graser, S. Jürgens, M. E. Wilhelm, M. Cokoja, W. A. Herrmann, F. E. Kühn, *Z. Naturforsch.* **2013**, *68b*, 1138 – 1142.
[63] B. Zhang, M. Köberl, A. Pöthig, M. Cokoja, W. A. Herrmann, F. E. Kühn, *Z. Naturforsch.* **2012**, *67b*, 1030 – 1036.
[64] B. Zhang, M.-D. Zhou, M. Cokoja, J. Mink, S. L. Zang, F. E. Kühn, *RSC Advances* **2012**, *2*, 8416 – 8420.
[65] S. A. Dharaskar, *Res. J. Chem. Sci.* **2012**, *2*, 80 – 85.
[66] I. V. Babich, J. A. Moulijn, *Fuel* **2003**, *82*, 607 – 631.
[67] K. Kaczorowska, Z. Kolarska, K. Mitka, P. Kowalski, *Tetrahedron* **2005**, *61*, 8315 – 8327.
[68] F. Brebion, B. Delouvrie, F. Najera, L. Fensterbank, M. Malacria, J. Vaissermann, *Angew. Chem. Int. Ed.* **2003**, *42*, 5342 – 5345.
[69] M. S. Chen, M. C. White, *J. Am. Chem. Soc.* **2004**, *126*, 1346 – 1347.
[70] E. Martin, D. L. Hughes, S. J. Lancaster, *Inorg. Chim. Acta* **2010**, *363*, 275 – 278.
[71] Y. Zhang, A. M. Santos, E. Herdtweck, J. Mink, F. E. Kühn, *New J. Chem.* **2005**, *29*, 366 – 370.
[72] A. R. Katritzky, S. Singh, K. Kirichenko, M. Smiglak, J. D. Holberey, W. M. Reichert, S. K. Spear, R. D. Rogers, *Chem. Eur. J.* **2006**, *12*, 4630 – 4641.
[73] J. Dymon, R. Wibby, J. Kleingardner, J. M. Tanski, I. A. Guzer, J. D. Holbrey, A. S. Larsen, *Dalton Trans.* **2008**, 2999 – 3006.
[74] T. Peppel, C. Roth, K. Fumino, D. Paschek, M. Möckerling, R. Ludwig, *Angew. Chem. Int. Ed.* **2011**, *50*, 6661 – 6663.
[75] K. Fumino, A. Wulf, R. Ludwig, *Angew. Chem. Int. Ed.* **2009**, *48*, 3184 – 3186.
[76] A. Wulf, K. Fumino, R. Ludwig, *Angew. Chem. Int. Ed.* **2010**, *49*, 449 – 453.
[77] B. E. Diebl, Y. Li, M. Cokoja, F. E. Kühn, N. Radhakrishnan, S. Zschoche, H. Komber, H. Y. Yeong, B. Voit, O. Nuyken, P. Hanefeld, H.-M. Walter, *J. Polym. Sci., Part A: Polym. Chem.* **2010**, *48*, 3775 – 3786.
[78] Y. Li, L. T. Voon, H. Y. Yeong, A. K. Hijazi, N. Radhakrishnan, K. Köhler, B. Voit, O, Nuyken, F. E. Kühn, *Chem. Eur. J.* **2008**, *14*, 7997 – 8003.
[79] A. K. Hijazi, N. Radhakrishnan, K. R. Jain, E. Herdtweck, O. Nuyken, H. M. Walter, P. Hanefeld, B. Voit, F. E. Kühn, *Angew. Chem. Int. Ed.* **2007**, *46*, 7290 – 7292.
[80] F. Schödel, H. W. Lerner, M. B. Roig, M. Bolte, *Acta Crystallogr.* **2006**, *E62*, 372 – 373.
[81] D. Brage, F. Grepioni, G. R. Desiraju, *Chem. Rev.* **1998**, *98*, 1375 – 1405.
[82] F. A. Cotton, K. J. Wiesinger, *Inorg. Chem.* **1991**, *30*, 871 – 873.
[83] P. G. Jones, O. Crespo, *Acta Crystallogr., Sect. C: Cryst. Struct. Commun.* **1998**, *54*, 18 – 20.
[84] N. Kuhn, M. Walker, M. Steimann, *Z. Naturforsch.* **2002**, *57b*, 248 – 250.
[85] M. Köberl, M. Cokoja, B. Bechlars, E. Herdtweck, F. E. Kühn, *Dalton Trans.* **2011**, *40*, 11490 – 11496.
[86] K. Kaczorowska, Z. Kolarska, K. Mitka, P. Kowalski, *Tetrahedron* **2005**, *61*, 8315 – 8327.
[87] J. Drabowicz, M. Mikolajczyk, *Synth. Commun.* **1981**, *11*, 1025 – 1030.
[88] W. L. Xu, Y. Z. Li, Q. S. Zhang, H. S. Zhu, *Synthesis* **2004**, 227 – 232.

[89] V. Hulea, P. Mordau, F. D. Renzo, *J. Mol. Catal. A: Chem.* **1996**, *111*, 325 – 332.
[90] K. S. Ravikumar, F. Barbier, J. P. Bégué, D. B. Delpon, *J. Fluorine Chem.* **1999**, *95*, 123 – 125.
[91] J. Dupont, R. F. de Souza, P. A. Z. Suarez, *Chem. Rev.* **2002**, *102*, 3667 – 3692.
[92] J. W. Wiench, C. Michon, A. Ellern, P. Hazendonk, A. Luga, R. J. Angelici, M. Pruski, *J. Am. Soc. Chem.* **2009**, *131*, 11801 – 11810.
[93] C. Wamser, *J. Am. Soc. Chem.* **1951**, *73*, 409 – 416.
[94] I. Bányai, V. Conte, L. Pettersson, A. Silvagni, *Eur. J. Inorg. Chem.* **2008**, 5373 – 5381.
[95] K. Kwon, J. Park, C. K. Lee, H. Kim, *Int. J. Electrochem. Sci.* **2012**, *7*, 9835 – 9843.
[96] Y. S. Li, R. A. Larsen, F. O. Cox, J. R. Durig, *J. Raman Spectrosc.* **1989**, *20*, 1 – 9.
[97] J. Mihály, S. Sterkel, H. M. Ortner, L. Kocsis, L. Hajba, É. Furdyga, J. Mink, *Croat. Chem. Acta* **2006**, *79*, 497 – 501.
[98] S. Eltayeb, G. A. Guirgis, A. R. Fanning, J. R. Durig, *J. Raman Spectrosc.* **1996**, *27*, 111 – 126.
[99] J. Murto, A. Kivinen, K. Kajander, J. Hyömäki, J. K. Tommola, *Acta Chem. Scand.* **1973**, *27*, 96 – 106.
[100] B. C. Matusewicz, S. Pilorz, D. Bieńko, D. Michalska, *Vib. Spectrosc.* **2008**, *47*, 44 – 52.
[101] J. F. Kang, A. Ulman, R. Jordan, *Langmuir* **1999**, *15*, 5555 – 5559.
[102] U. Lappan, U. Geißler, U. Scheler, K. Lunkwitz, *Radiat. Phys. Chem.* **2003**, *67*, 447 – 451.
[103] W. Grochala, M. K. Cytańskl, M. Derzsl, T. Michalowkl, P. J. Malinowski, Z. Mazej, D. Kurzydlowski, W. Koźmiński, A. Budzianowski, P. J. Leszyński, *Dalton Trans.* **2012**, *41*, 2034 – 2047.
[104] N. P. G. Roeges, A guide to the complex interpretation of infrared spectra of organic structures, John Wiley & Sons, Chichester, **1994**, 29 – 40.
[105] APEX suite of crystallographic software, APEX 2 (version 2008.4), Bruker Analytical X-ray Instruments Inc., Madison, Wisconsin (USA) **2008**.
[106] SAINT (version 7.56a), SADABS (version 2008/1). Bruker Analytical X-ray Instruments Inc., Madison, Wisconsin (USA) **2008**.
[107] L. J. Farrugia, *J. Appl. Crystallogr.* **1999**, *32*, 837 – 838.
[108] A. Altomare, G. Cascarano, C. Giacovazzo, A. Gugliardi, M. C. Burla, G. Polidori, M. Camalli, *J. Appl. Crystallogr.* **1994**, *27*, 435.
[109] G. M. Sheldrick, *Acta Crystallogr.* **2008**, *A64*, 112 – 122.
[110] A. J. C. Wilson (Ed.), *International Tables for Crystallography*, Vol. C, Kluwer Academic Publishers, Dordrecht, **1992**, Tables 6.1.1.4 (pp. 500 – 502), 4.2.6.8 (pp. 219 – 222), and 4.2.4.2 (pp. 193 – 199).
[111] A. L. Spek, *Acta Crystallogr.* **2009**, *D65*, 148 – 155.